m, 4 H). UV-vis (CH_2Cl_2): λ 416 (Soret), 535, 567 nm. IR (CH_2Cl_2): CO stretch 1951 cm^{-1}.

Summary

The picnic-basket porphyrins are readily available via a convergent, general synthesis. These tetraarylporphyrins bear rigid organic appendages that define a molecular cavity on one face of the porphyrin macrocycle. The large cavity volume of the hexyl-bridged picnic-basket porphyrin has been confirmed by X-ray crystallographic analysis and by ligand-binding studies. The utility of these protected porphyrins as cytochrome P-450 active-site analogues is currently being explored.

Acknowledgment. Support from the National Institutes of Health (Grants NIH GM17880-16 and NIH GM17880-17 to J.P.C. and Grant NIH HL-13157 to J.A.I.) and the National Science Foundation (Grant NSF CHE83-18512 to J.P.C.) is gratefully acknowledged. The Nicolet NMC-300 and Varian XL-400 spectrometers were purchased with funds from the National Science Foundation (Grants NSF CHE81-09064 and NSF CHE84-14329). Ms. Patricia Bethel and the University of California, San Francisco Mass Spectrometry Facility supported by the National Institutes of Health (Grant RR01614) obtained all the mass spectral data reported. Mr. Ronald Nelson is gratefully acknowledged for synthetic help. We thank Dr. Robert Hembre for help in preparing the manuscript.

Registry No. 2a, 113585-29-8; **2b**, 52739-96-5; **2c**, 113585-30-1; **2d**, 113585-31-2; **2e**, 113585-32-3; **2f**, 113585-33-4; **2g**, 113597-93-6; **2h**, 113585-34-5; **3a**, 52739-95-4; **3b**, 113585-35-6; **3c**, 22937-73-1; **3d**, 113585-36-7; **3e**, 22937-74-2; **3f**, 22937-70-8; **3g**, 113585-37-8; **3h**, 113585-38-9; **4a**, 113585-39-0; **4b**, 113585-40-3; **4c**, 113597-94-7; **4d**, 113597-95-8; **4e**, 113597-96-9; **4f**, 113585-41-4; **4g**, 113585-42-5; **4h**, 113585-43-6; **5a**, 113597-97-0; **5b**, 113597-98-1; **5c**, 113585-44-7; **5d**, 113585-45-8; **5e**, 113585-46-9; **5f**, 113585-47-0; **5g**, 113585-48-1; **5h**, 113585-49-2; **6**, 36596-67-5; **7**, 113585-50-5; **8**, 113597-99-2; **9**, 113598-00-8; **10**, 113585-10-7; **11**, 113585-11-8; **12**, 113585-12-9; **13**, 113585-13-0; **14**·$4C_5H_5N$, 113666-12-9; 4:0 TAMPP, 52199-35-6; $Br(CH_2)_2Br$, 106-93-4; $Br(CH_2)_4Br$, 110-52-1; $Br(CH_2)_6Br$, 124-09-4; $Br(CH_2)_8Br$, 373-44-4; $Br(CH_2)_{10}Br$, 646-25-3; $Ru_3(CO)_{12}$, 15243-33-1; 1,4-bis(bromomethyl)benzene, 623-24-5; diethyl 5-hydroxyisophthalate, 39630-68-7; 5-hydroxyisophthalic acid, 618-83-7; bis(diphenylmethyl) 5-hydroxyisophthalate, 113585-51-6; diphenyldiazomethane, 883-40-9; 2,6-dimethylbenzoic acid, 632-46-2; 1,1'-binaphth-2-ol, 602-09-5.

Supplementary Material Available: Bond distances (Table 1S), bond angles (Table 2S), dihedral angles (Table 3S), displacements from the mean porphyrin plane (Table 4S), distances between O (of CO) and the basket atoms (Table 5S), positional and thermal parameters for the non-hydrogen atoms (Table 6S), positional and thermal parameters of the hydrogen atoms (Table 7S), anisotropic thermal parameters (Table 8S) (16 pages); structural amplitudes (Table 9S) (46 pages). Ordering information is given on any current masthead page.

Reversible Binding of Dinitrogen and Dioxygen by a Ruthenium "Picnic-Basket" Porphyrin

James P. Collman,*† John I. Brauman,† Jeffrey P. Fitzgerald,† John W. Sparapany,‡ and James A. Ibers†

Contribution from the Department of Chemistry, Stanford University, Stanford, California 94305, and Department of Chemistry, Northwestern University, Evanston, Illinois 60208. *Received July 8, 1987*

Abstract: We recently reported the synthesis and characterization of ruthenium "picnic-basket" porphyrin carbonyl complexes. These synthetic tetraarylporphyrins bear a rigid superstructure that defines a molecular cavity on one face of the porphyrin macrocycle. Photolysis of these carbonyl complexes in a coordinating solvent results in formation of bis-solvent complexes. The bis(pyridine) complex has been structurally characterized. General methods to control axial ligation in these ruthenium picnic-basket porphyrins are presented. A transient pentacoordinate ruthenium picnic-basket porphyrin, which reversibly binds both dinitrogen and dioxygen within the protected cavity, has been prepared. The N_2 and O_2 complexes have been characterized by UV-visible, ^1H NMR, and IR spectroscopies. The diamagnetic dioxygen complex shows $\nu(^{16}O-^{16}O)$ at 1103 cm^{-1} and thus is described as containing coordinated superoxide ion. A correlation between dioxygen binding and the Ru(III/II) potential was observed.

Interactions between molecular oxygen and low-valent metalloporphyrins have received considerable attention because of their relevance to the biological transport and activation of oxygen by hemoproteins.[1] The periodic relationship of ruthenium to iron, the metal found in hemoproteins, has stimulated considerable interest in the interactions of ruthenium porphyrins and molecular oxygen. To date, however, no example of a well-characterized ruthenium porphyrin dioxygen adduct has been reported.

The first ruthenium porphyrin reported to bind dioxygen reversibly was a five-coordinate ruthenium(II) porphyrin pyridine complex, stabilized within a lipid monolayer.[2] Hopf and Whitten formed this species by photochemical ejection of CO from the six-coordinate carbonyl adduct that had already been incorporated in the monolayer. Prior to this, all known ruthenium(II) porphyrins were six-coordinate and contained strong π-acceptor ligands that render the ruthenium(II) center inert to dioxygen.[3] The five-coordinate species was also reported to bind dinitrogen reversibly. Unfortunately, because of the lipid matrix the only

†Stanford University.
‡Northwestern University.

(1) (a) Vaska, L. *Acc. Chem. Res.* **1976**, *9*, 175-183. (b) Jones, R. D.; Summerville, D. A.; Basolo, F. *Chem. Rev.* **1979**, *79*, 139-179. (c) Basolo, F.; Hoffman, B. M.; Ibers, J. A. *Acc. Chem. Res.* **1975**, *8*, 384-392. (d) Collman, J. P. *Acc. Chem. Res.* **1977**, *10*, 265-272. (e) Summerville, D. A.; Jones, R. D.; Hoffman, B. M.; Basolo, F. *J. Chem. Educ.* **1979**, *56*, 157-162. (f) Mlodnicka, T. *J. Mol. Catal.* **1986**, *36*, 205-242.

(2) Hopf, F. R.; Whitten, D. G. *J. Am. Chem. Soc.* **1976**, *98*, 7422-7424.

(3) (a) Fleischer, E. B.; Thorp, R.; Venerable, D. *J. Chem. Soc., Chem. Commun.* **1969**, 475. (b) Chow, B. C.; Cohen, I. A. *Bioinorg. Chem.* **1971**, *1*, 57-63. (c) Tsutsui, M.; Ostfeld, D.; Hoffman, L. M. *J. Am. Chem. Soc.* **1971**, *93*, 1820-1823. (d) Tsutsui, M.; Ostfeld, D.; Francis, J. N.; Hoffman, L. N. *J. Coord. Chem.* **1971**, *1*, 115-119. (e) Little, R. G.; Ibers, J. A. *J. Am. Chem. Soc.* **1973**, *95*, 8583-8590. (f) Bonnet, J. J.; Eaton, S. S.; Eaton, G. R.; Holm, R. H.; Ibers, J. A. *J. Am. Chem. Soc.* **1973**, *95*, 2141-2149.

0002-7863/88/1510-3486$01.50/0

Scheme I. Reactions between Labile Ruthenium(II) Porphyrin Complexes and Molecular Oxygen

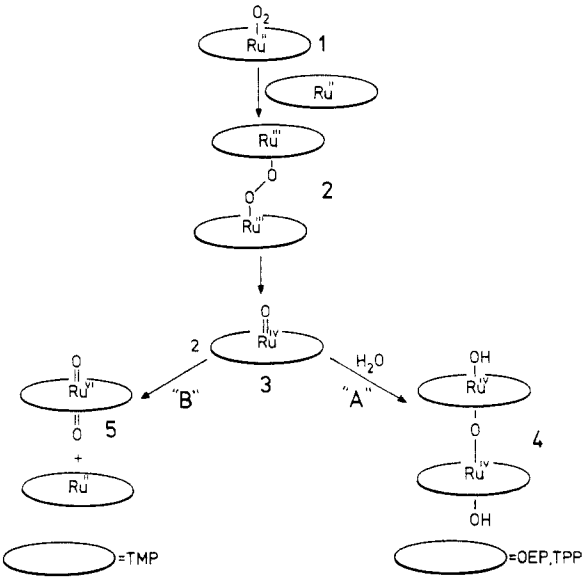

method of characterizing these interesting species was UV–visible spectroscopy.

Dolphin, James, and co-workers also recognized the potential of ruthenium(II) porphyrins to bind dioxygen reversibly. They reported that $Ru(OEP)(CH_3CN)_2$, dissolved in polar, weakly coordinating solvents, such as DMF or pyrrole, readily absorbed 1 equiv of dioxygen.[4] Under vacuum, the absorbed dioxygen could be removed, regenerating the ruthenium starting material. On the basis of its unusual visible spectrum and by analogy to the known ethylene complex, they speculated that their new ruthenium complex contained η^2-bound dioxygen reduced to the level of peroxide. Formation of this new species was found to depend critically on the choice of starting material and solvent. Treatment of either a DMF solution of $Ru(OEP)L_2$ (L = pyridine or 1-methylimidazole) or a toluene solution of $Ru(OEP)(CH_3CN)_2$ with oxygen gas led to irreversible decomposition. The decomposition product was shown to contain approximately 0.25 mol of O_2 per mol of ruthenium but was not further identified.

Collman et al. observed similar irreversible oxidations when dimers of ruthenium(II) octaethylporphyrin and tetraphenylporphyrin were exposed to molecular oxygen.[5] Here, however, the oxidation products were identified as hydroxy-capped μ-oxo dimers of Ru(IV). This assignment was based on complete spectral characterization and a crystal structure of the oxo-bridged species prepared by an alternate route.[6]

In contrast to the above products, dioxygen reacts with labile ruthenium derivatives of the sterically demanding tetramesitylporphyrin to give $Ru^{VI}(TMP)(O)_2$.[7,8] The diamagnetic ruthenium(VI) species, which contains two axial oxo ligands, has been characterized by visible, infrared, and ^1H NMR spectroscopies.[9] The bulky mesitylporphyrin substituents are necessary to prevent two ruthenium centers from approaching close enough to form a μ-oxo bridge.

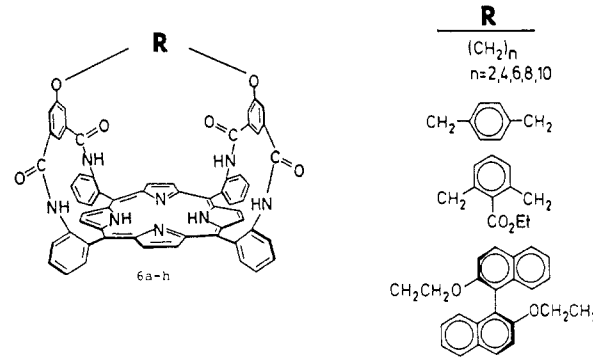

Figure 1. The "picnic-basket" porphyrins.

These irreversible oxidations of ruthenium(II) porphyrins, by analogy to the autoxidation of ferrous porphyrins,[10] are believed to occur by the mechanism outlined in Scheme I. An initially formed dioxygen adduct, **1**, reacts with a second equivalent of low-valent ruthenium porphyrin to form a μ-peroxo bridged dimer, **2**, that homolytically cleaves the O–O bond to give 2 equiv of an oxoruthenium(IV) species, **3**. If the porphyrin ligand is sterically unencumbered (i.e., OEP, TPP), then redimerization of the ruthenium(IV) species via a bridging oxo ligand and reaction with 1 equiv of water gives the hydroxy-capped product, **4** (path A). If formation of the oxo bridge is sterically prevented by a bulky porphyrin ligand (i.e., TMP), then reaction with a second equivalent of dioxygen occurs to give the ruthenium(VI) dioxo complex, **5**. Groves and Quinn have proposed this occurs through disproportionation of two oxoruthenium(IV) via a transient μ-oxo dimer to produce a ruthenium(VI) dioxo and a ruthenium(II) porphyrin that can react with more O_2 (path B).[7]

Thus, in order to isolate a stable dioxygen complex of a ruthenium porphyrin, formation of the μ-peroxo species must be prevented. A method that has been used successfully to stabilize dioxygen adducts of ferrous porphyrins is to bind the O_2 molecule within a sterically encumbered environment; this prevents the dimerization reaction that leads to irreversible oxidative decomposition.[11]

The picnic-basket porphyrins (**6a–h**), illustrated in Figure 1, are a series of synthetic tetraarylporphyrins that contain a rigid superstructure on one face of the porphyrin macrocycle.[12] The superstructure consists of two isophthalate rings, each joined to the porphyrin ring by two amide linkages and joined to each other by a bridging group, R. The cavity defined by this superstructure may be varied in size, functionality, and chirality by changing the bridging group. Various derivatives of these picnic-basket porphyrins are specified by the notation $M(R\text{-}PBP)(L)_{in}(L')_{out}$, where M = metal or H_2 for unmetalated porphyrins, R = bridging group (C*n* = *n*-methylene alkane, PXY = *p*-xylene, DMB = 2,6-dimethylbenzoate, BN = binaphthyl), PBP = picnic-basket porphyrin, $(L)_{in}$ = ligand coordinated within protected cavity, and $(L')_{out}$ = ligand bound on unencumbered porphyrin face.

We recently reported the synthesis and characterization of ruthenium carbonyl complexes of several picnic-basket porphyrins.[12] To the best of our knowledge, these are the first cavity-containing porphyrins to be metalated with ruthenium.[13] Thus,

(4) (a) Farrell, N.; Dolphin, D.; James, B. R. *J. Am. Chem. Soc.* **1978**, *100*, 324–326. (b) James, B. R.; Addison, A. W.; Cairns, M.; Dolphin, D.; Farrell, N. P.; Paulson, D. R.; Walker, S. *Fundamental Research in Homogeneous Catalysis*; Tsutsui, M., Ed.; Plenum: New York, 1979; Vol. 3, pp 751–772. (c) Smith, P. D.; James, B. R.; Dolphin, D. H. *Coord. Chem. Rev.* **1981**, *39*, 31–75.

(5) (a) Collman, J. P.; Barnes, C. E.; Collins, T. J.; Brothers, P. J.; Gallucci, J.; Ibers, J. A. *J. Am. Chem. Soc.* **1981**, *103*, 7030–7032. (b) Collman, J. P.; Barnes, C. E.; Swepston, P. N.; Ibers, J. A. *J. Am. Chem. Soc.* **1984**, *106*, 3500–3510.

(6) (a) Masuda, H.; Taga, T.; Osaki, K.; Sugimoto, H.; Mori, M.; Ogoshi, H. *J. Am. Chem. Soc.* **1981**, *103*, 2199–2203. (b) Collman, J. P.; Barnes, C. E.; Brothers, P. J.; Collins, T. J.; Ozawa, T.; Gallucci, J.; Ibers, J. A. *J. Am. Chem. Soc.* **1984**, *106*, 5151–5163.

(7) Groves, J. T.; Quinn, R. *J. Am. Chem. Soc.* **1985**, *107*, 5790–5792.

(8) Camenzind, M. J.; James, B. R.; Dolphin, D. H. *J. Chem. Soc., Chem. Commun.* **1986**, 1137–1139.

(9) Groves, J. T.; Quinn, R. *Inorg. Chem.* **1984**, *23*, 3844–3846.

(10) (a) Hammond, G. S.; Wu, C. S. *Adv. Chem. Ser.* **1968**, *77*, 186–207. (b) Alben, J. O.; Fuchsman, W. H.; Beaudreau, C. A.; Caughey, W. S. *Biochemistry* **1968**, *7*, 624–635. (c) Cohen, I. A.; Caughey, W. S. *Biochemistry* **1968**, *7*, 636–641. (d) Sadasivan, N.; Eberspraecher, H. J.; Fuchsman, W. H.; Caughey, W. S. *Biochemistry* **1969**, *8*, 534–541. (e) Balch, A. L.; Chan, Y.-N.; Cheng, R.-J.; La Mar, G. N.; Latos-Grazynski, L.; Renner, M. W. *J. Am. Chem. Soc.* **1984**, *106*, 7779–7785. (f) Hoffman, A. B.; Collins, D. M.; Day, V. W.; Fleischer, E. B.; Srivastava, T. S.; Hoard, J. L. *J. Am. Chem. Soc.* **1972**, *94*, 3620–3626.

(11) Suslick, K. S.; Reinert, T. J. *J. Chem. Educ.* **1985**, *62*, 974–983.

(12) Collman, J. P.; Brauman, J. I.; Fitzgerald, J. P.; Hampton, P. D.; Naruta, Y.; Sparapany, J. W.; Ibers, J. A. *J. Am. Chem. Soc.*, previous paper in this issue.

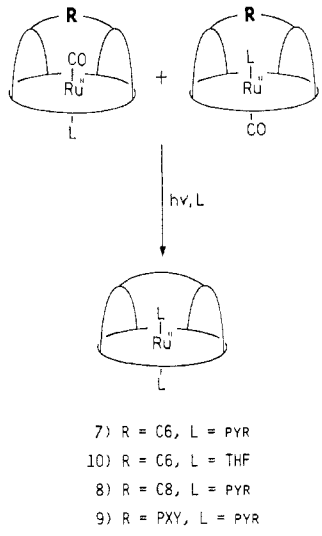

Figure 2. Photochemical CO ejection from ruthenium picnic-basket porphyrin complexes.

Table I

	pyridine 1			pyridine 2		
porphyrin	H_o	H_m	H_p	H_o	H_m	H_p
C6-PBP	2.95	5.39	6.25	1.68	4.03	4.63
C8-PBP	2.86	5.36	6.22	1.89	3.78	4.84
PXY-PBP	2.95	5.37	6.23	1.56	3.41	2.51
TPP	2.47	5.19	6.01			

these ruthenium picnic-basket porphyrins provide a unique opportunity to stabilize a ruthenium porphyrin dioxygen complex, assuming dioxygen can be bound within the protected pocket.

We report herein the synthesis and characterization, including a crystal structure, of bis(pyridine) and bis(tetrahydrofuran) complexes of several picnic-basket porphyrins. Selected aspects of their coordination chemistry are discussed. Methods for controlling the regiochemistry of axial ligation in ruthenium picnic-basket porphyrin complexes are presented. Application of these methods has resulted in the synthesis of both dinitrogen and dioxygen adducts of a ruthenium picnic-basket porphyrin; each has been characterized by a range of spectral techniques.

Results and Discussion

Carbonyl Replacement. We previously reported the synthesis and characterization of several ruthenium(II) picnic-basket porphyrin carbonyl complexes.[12] Ruthenium(II) porphyrins are strongly stabilized by the back-bonding carbonyl ligand, which must be removed in order to observe reactions with weaker π-acid ligands. Two methods have been reported for removal of the carbonyl ligand from a ruthenium porphyrin. The first is photochemical ejection of CO in the presence of a coordinating ligand[14] and the second is an oxidative method.[6] For the purpose of these studies the photochemical method was preferred because the product remains a ruthenium(II) porphyrin.

Photolysis of either regioisomer or more commonly the mixture of Ru(C6-PBP)(CO)(pyr) isomers in degassed pyridine resulted in loss of the carbonyl ligand and formation of the ruthenium(II) bis(pyridine) complex, **7**, as illustrated in Figure 2. The bis(pyridine) complexes of Ru(C8-PBP), **8**, and Ru(PXY-PBP), **9**, were prepared in a similar manner. These air-stable compounds are soluble in polar aprotic solvents and are easily purified by silica gel chromatography.

As with the carbonyl complexes, ^{1}H NMR spectroscopy has proven particularly useful in characterizing these diamagnetic bis(pyridine) species. Spectral analysis shows two types of coordinated pyridine. The pyridine chemical shifts for the three Ru(PBP)(pyr)$_2$ complexes and the related tetraphenylporphyrin derivative[15] are listed in Table I. Chemical shifts for one type of pyridine were observed to be independent of the picnic-basket porphyrin structure and are assigned to pyridine coordinated on the unhindered side of the porphyrin. Supporting this assignment are the similar chemical shifts observed for pyridine in the related tetraphenylporphyrin species. Signals for the other type of coordinated pyridine were observed at higher field and are dependent on the picnic-basket porphyrin superstructure, indicative of pyridine coordination within the pocket. An upfield shift for ligands coordinated within the cavity is expected because of the anisotropic shielding of the isophthalamido rings.

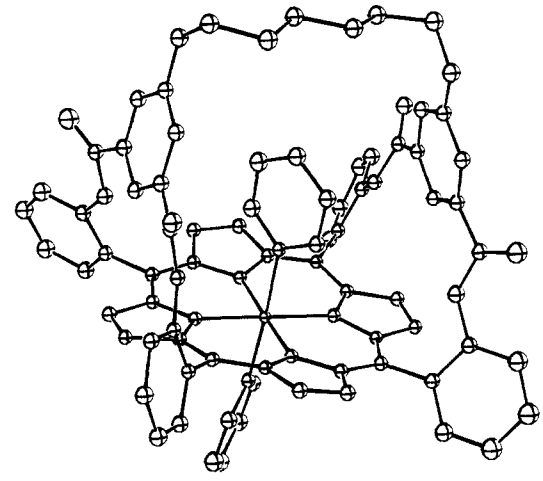

Figure 3. Molecular structure of Ru^{II}(C6-PBP)(pyr)$_2$.

Photolysis of an argon-purged THF solution of Ru(C6-PBP)(CO)$_{out}$(THF)$_{in}$ similarly results in formation of the bis(tetrahydrofuran) adduct, **10**. No reaction was observed when the above reaction was carried out in a sealed tube, a procedure that works smoothly to form the bis(pyridine) complex. The argon purge is apparently necessary to remove the liberated CO. Ru(C6-PBP)(THF)$_2$ is only slightly soluble in less polar organic solvents but is readily dissolved in more polar solvents such as THF. In the absence of excess THF, this material readily reacts with dioxygen or chlorinated hydrocarbons. As with the bis(pyridine) analogue, two types of coordinated THF are observed in the ^{1}H NMR spectrum of a toluene-d_8 solution. Again, comparison of chemical shifts for the coordinated THF in this molecule and in the TPP derivative indicates that one THF is bound within the pocket and another on the open face of the picnic-basket porphyrin. Examination of the ^{1}H NMR spectrum of Ru(C6-PBP)(THF)$_2$ in THF-d_8 showed 1 equiv of bound THF, coordinated within the pocket, and 1 equiv of free THF that presumably was displaced by the deuteriated solvent. This phenomenon will be discussed later.

Interestingly, all attempts to remove the carbonyl ligand from within the ethyl-bridged pocket by photolysis were unsuccessful. Irradiation of a pyridine, THF, or acetonitrile solution of Ru(C2-PBP)(CO)$_{in}$(pyr)$_{out}$ in a sealed tube resulted in no reaction. Irradiation of any of these solutions when purged with argon resulted in formation of an uncharacterized blue-green material. Examination of CPK models shows that neither pyridine nor THF can fit into the C2-PBP pocket and that acetonitrile would suffer serious steric interactions when coordinated within the cavity of this porphyrin. Formation of an uncharacterized green compound was observed by Brothers and Collman[16] during photolysis of the ruthenium pocket porphyrin carbonyl complex. Thus, the photolytic replacement of CO is extremely sensitive to the cavity size.

X-ray Structure of Ru(C6-PBP)(pyr)$_2$. Suitable crystals for X-ray analysis were obtained by room-temperature vapor diffusion

(13) Recently a cofacial dimer of ruthenium porphyrins has been reported (Collman, J. P.; Kim, K. K.; Garner, J. M. *J. Chem. Soc., Chem. Commun.* **1986**, 1711–1713).

(14) Sovocool, G. W.; Hopf, F. R.; Whitten, D. G. *J. Am. Chem. Soc.* **1972**, *94*, 4350–4351.

(15) Antipas, A.; Buchler, J. W.; Gouterman, M.; Smith, P. D. *J. Am. Chem. Soc.* **1978**, *100*, 3015–3024.

(16) Brothers, P. J.; Collman, J. P., unpublished observations.

Table II. Crystallographic Data for Ru(C6-PBP)(pyr)$_2$·2pyr·2tol

formula	$RuC_{76}H_{56}N_{10}O_6 \cdot 2C_5H_5N \cdot 2C_7H_8$
formula wt, amu	1647.9
space group	C_{2h}^5–$P2_1/n$
a, Å	13.451 (5)
b, Å	24.77 (1)
c, Å	24.62 (1)
β, deg	105.25 (3)
V, Å^3	7948
Z	4
temp, °C	−150 (1)[a]
radiation	Mo Kα, λ(Kα$_1$) = 0.70930 Å graphite monochromator
linear absorp coeff, cm^{-1}	2.57
transmission factors	0.895–0.947[b]
density (calcd), g/cm^3	1.377
crystal vol, mm^3	0.0659
detector aperture	2 mm high × 2 mm wide 17.3 cm from crystal
take-off angle, deg	2.3
scan mode	ω
scan speed	2° in ω; reflections having $F_o^2 < 3\sigma(F_o^2)$ were rescanned to achieve a 3σ level up to a maximum scan time of 100 s
scan range, deg	±0.8 in ω
2θ limits, deg	$2 < 2\theta < 50$
background counts	1/4 of scan range on each side of reflection
data collected	±h,+k,+l
standard reflections	6 in diverse regions of reciprocal space remeasured every 3.0 h of X-ray exposure time
unique data (including $F_o^2 < 0$)	14266
unique data ($F_o^2 > 3\sigma(F_o^2)$)	11925
final no. of variables	473
p factor for $\sigma(F_o^2)$	0.03
$R(F)$ ($F_o^2 > 3\sigma(F_o^2)$)	0.060
$R_w(F)$ ($F_o^2 > 3\sigma(F_o^2)$)	0.075
error in observation of unit weight, e^2	2.87

[a] The low-temperature system is from a design by Prof. J.-J. Bonnet and S. Askinazy and is commercially available from Solerem, Z. I. de Vic, 31320 Castanet-Tolosan, France. [b] The analytical method, as employed in the Northwestern absorption program AGNOST, was used for the absorption correction (de Meulenaer, J.; Tompa, H. *Acta Crystallogr.* **1965**, *19*, 1014–1018).

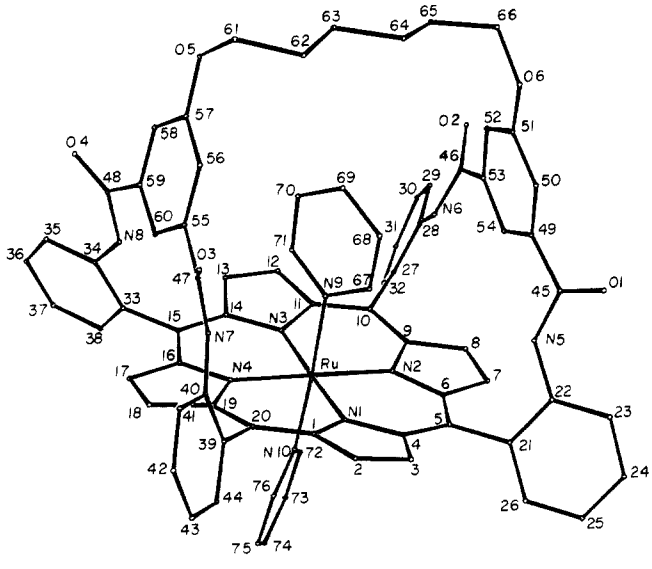

Figure 4. Numbering scheme for Figure 3.

of toluene into a pyridine solution of Ru(C6-PBP)(pyr)$_2$ over 2 weeks. This molecule crystallizes with two toluene and two pyridine solvate molecules. Crystal data and collection procedures are listed in Table II. The molecular structure is shown in Figure 3 and the numbering scheme in Figure 4. Key bond lengths and angles for the picnic-basket porphyrin complex and the structurally characterized octaethylporphyrin derivative[17] are listed in Table III. More complete bond distances and bond angles are given in Tables 1S and 2S.[18] Tables 3S and 4S[18] provide metrical data for the toluene and pyridine solvate molecules.

Table III. Averaged Bond Lengths (Å) and Angles (Deg) for Some Ruthenium Porphyrin Bis(pyridine) Complexes

	Ru(C6-PBP)(pyr)$_2$	Ru(OEP)(pyr)$_2$[16]
Ru–N(pyr)$_{in}$	2.117 (4)[a]	2.089 (6), 2.100 (6)[c]
Ru–N(pyr)$_{out}$	2.097 (4)	
Ru–N(porph)	2.037 (7)[b]	2.036 (10)
N–C$_a$	1.382 (5)	1.378 (9)
C$_a$–C$_m$	1.401 (5)	1.37 (2)
C$_a$–C$_b$	1.445 (5)	1.47 (2)
C$_b$–C$_b$	1.351 (5)	1.37 (1)
C$_a$–N–C$_a$	106.5 (3)	107.5 (6)
N–C$_a$–C$_b$	109.4 (3)	109.3 (8)
N–C$_a$–C$_m$	125.3 (3)	125.0 (9)
C$_a$–C$_b$–C$_b$	107.4 (3)	107.2 (9)
C$_a$–C$_m$–C$_a$	125.3 (6)	127.2 (8)
N(pyr)–Ru–N(pyr)	177.5 (1)	180

[a] Data collected at −150 °C. [b] This error in a mean value is the larger of the unweighted estimated standard deviation of a single observation as estimated from the value averaged or as estimated from the least-squares inverse matrix. [c] Data collected presumably at room temperature.

The large volume of the hexyl-bridged cavity is evident in that no distortion of pyridine bound within the pocket is observed. Distances from the pyridine within the pocket to "basket" atoms are all greater than 3.8 Å (Table 5S).[18] In fact, the bond to pyridine within the cavity, 2.117 (4) Å, is slightly longer than to pyridine coordinated on the open porphyrin face, 2.097 (4) Å. These are very similar to the ruthenium–pyridine bond lengths of 2.089 (6) and 2.100 (6) Å reported for Ru(OEP)(pyr)$_2$ (Table III).[17] The pyridine ring bound within the pocket defines a plane that is perpendicular to the mean porphyrin plane (dihedral angle = 90.69°) while the plane of the pyridine bound outside the pocket is tipped relative to the mean plane of the porphyrin ring (dihedral angle = 96.81°). This may be due to crystal packing forces. The planes defined by each pyridine ring intersect at a dihedral angle of 113°. This is very different from the centrosymmetric Ru(OEP)(pyr)$_2$ in which the two pyridine rings are coplanar. As in the ruthenium carbonyl pyridine complex, the porphyrin ring in Ru(C6-PBP)(pyr)$_2$ is distorted (Tables 7S and 8S).[18] The distortion has approximate C_2 symmetry, the maximum displacement from the mean porphyrin plane being 0.33 Å (Table 8S).[18]

Ligand Dissociation Kinetics. Our eventual goal of coordinating dioxygen within the picnic-basket porphyrin cavity requires some knowledge of ligand labilities in these ruthenium picnic-basket porphyrin complexes. We therefore sought to measure the ligand dissociation rate constants for Ru(C6-PBP)(L)$_2$ (L = pyridine or THF).

Two methods were used to measure the rate of pyridine dissociation from the bis(pyridine) complex. The first is a modified literature procedure and monitors the visible spectral changes as the bis(pyridine) adduct reacts with excess isocyanide.[19] The second method involved preparing a solution of the bis(pyridine) complex in pyr-d_5 and monitoring the decay of the NMR signals for coordinated protiopyridine as it is replaced by the deuteriated solvent.

Treatment of an *o*-dichlorobenzene solution of Ru(C6-PBP)(pyr)$_2$ with excess benzyl isocyanide results in quantitative

(17) Hopf, F. R.; O'Brien, T. P.; Scheidt, W. R.; Whitten, D. G. *J. Am. Chem. Soc.* **1975**, *97*, 277–281.
(18) Supplementary material.
(19) (a) Eaton, S. S.; Eaton, G. R.; Holm, R. H. *J. Organomet. Chem.* **1971**, *32*, C52–C54. (b) Eaton, S. S.; Eaton, G. R.; Holm, R. H. *J. Organomet. Chem.* **1972**, *39*, 179–195. (c) Holloway, C. E.; Stynes, D. V.; Vuik, C. P. J. *J. Chem. Soc., Dalton Trans.* **1982**, 95–101. (d) Pomposo, F.; Carruthers, D.; Stynes, D. V. *Inorg. Chem.* **1982**, *21*, 4245–4248.

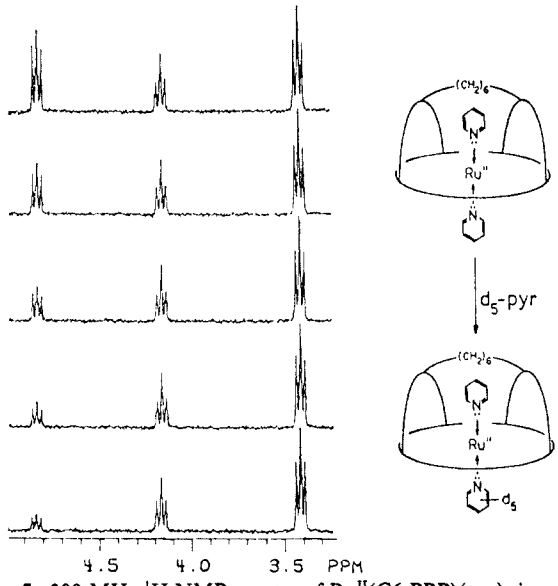

Figure 5. 300-MHz ^{1}H NMR spectra of Ru^{II}(C6-PBP)(pyr)$_2$ in pyr-d_5 at 90 °C (20 min between spectra).

formation of the bis(isocyanide) complex. Isosbestic points at 489, 518, and 637 nm indicate that this reaction proceeds without detectable intermediates. Replacement of the first axial pyridine by an isocyanide, which has a strong trans effect, labilizes the remaining pyridine. Analysis of the spectral changes as a function of time shows the first-order rate dependence on the ruthenium starting material concentration. Change of the initial benzyl isocyanide concentration over a factor of 5 caused no change in the observed rate. These observations are consistent with pyridine dissociation being rate limiting, and thus the pyridine dissociation rate constants can be measured directly. Although these experiments demonstrated the dissociative nature of ligand exchange in these systems, no information was obtained on which pyridine, inside or outside the hexyl-bridged pocket, was dissociating.

NMR spectroscopy allows us to distinguish, as mentioned above, ligands bound within the picnic-basket porphyrin cavity from those bound on the unencumbered face of the porphyrin. Figure 5 shows the changes observed in the ^{1}H NMR spectrum of Ru(C6-PBP)(pyr)$_2$ in pyr-d_5 thermostated at 90 °C. The two triplets at 4.17 and 3.42 ppm, in a 1:2 ratio, are assigned to the para and meta protons of pyridine within the pocket. The triplet at 4.84 ppm is due to the meta protons on pyridine coordinated on the open porphyrin face. This pyridine is completely replaced by the deuteriated solvent before the ligand inside the cavity has exchanged to any detectable extent. In fact, in order to observe replacement of the latter pyridine at measurable rates, a temperature of 130 °C is required. For both types of pyridine, exchange is observed to be a first-order process, consistent with pyridine dissociation being rate limiting.

Rate constants for THF dissociation from Ru(C6-PBP)(THF)$_2$ were measured similarly in THF-d_8. Unfortunately only a lower limit could be established for THF dissociation from the unhindered porphyrin face because complete exchange occurs in the 5 min between sample preparation and the first NMR spectrum.

Table IV lists the ligand dissociation rate constants that have been measured by this technique. As expected from ligand basicities, THF is much more labile than pyridine. However, two unexpected phenomena were observed. First, pyridine dissociation from the unhindered side of Ru(C6-PBP)(pyr)$_2$ is much slower than from Ru(TPP)(pyr)$_2$. A large reactivity difference was unexpected given the similar steric environment for pyridine in both positions. This reactivity difference may reflect differential stabilities in the five-coordinate intermediate or may be related to the unusually large difference in Ru(III/II) redox potential measured for these two molecules. The measured Ru(III/II) half-wave potential (vs SSCE) for Ru(C6-PBP)(pyr)$_2$ is 0.49 V while that of Ru(TPP)(pyr)$_2$ is 0.23 V. Saveant and associates[20] have ascribed unusually positive redox couples and high ligand affinities observed in amide-appended porphyrins to dipole effects.

Table IV. Rate Constants for Ligand Dissociation in Some Ruthenium Porphyrin Bis-Ligand Complexes

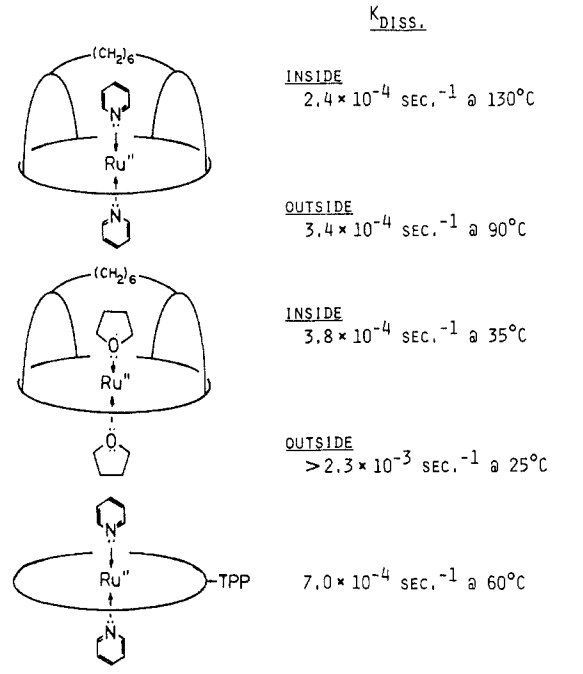

The second unusual result evident in Table IV is the much slower dissociation rates for ligands bound within the pocket compared to the same ligand bound outside the cavity. The lability difference for ligand inside versus outside the pocket is so large as to make measurement of both dissociation rate constants at the same temperture inconvenient by NMR methods.

The large reactivity difference could be due to greater stabilization of a ligand coordinated in the pocket, to destabilization of a putative five-coordinate complex that contains a free coordination site within the pocket, or to slow loss of ligand from the pocket. From our study of the interconversion of regioisomers of Ru(C6-PBP)(CO)(pyr) we know that the $(pyr)_{in}$ regioisomer is more stable than the $(pyr)_{out}$ by at least 2 kcal/mol. We propose this difference to result from a dipolar interaction with the porphyrin superstructure. This same dipolar effect could stabilize the ligand in the pocket, resulting in a slower dissociation rate. Alternatively, destabilizing a five-coordinate ruthenium complex that has a free coordination site in the pocket would result in a slower rate of ligand exchange. It is not obvious how the superstructure could have this effect. Finally, since a ligand within the cavity experiences steric interactions that could slow its rate of escape from the pocket, the effective higher local concentration of the ligand within the pocket could result in slower exchange rates. Attempts to determine activation parameters for ligand dissociation from inside and outside the porphyrin pocket have been so far unsuccessful.

Dinitrogen and Dioxygen Binding. In order to bind small gaseous molecules specifically within the picnic-basket porphyrin cavity, the unhindered face of the porphyrin must be blocked by a tightly coordinating, nonlabile ligand. Either no ligand, or a weakly held one, must occupy the coordination site within the pocket. The ligand dissociation rate constants determined above suggest that pyridine, or another strong base, will effectively block the open face of a ruthenium picnic-basket porphyrin at temperatures where THF, coordinated within the pocket, is very labile.

(20) (a) Lexa, D.; Momenteau, M.; Saveant, J.-M.; Xu, F. *J. Am. Chem. Soc.* **1986**, *108*, 6937–6941. (b) Lexa, D.; Rentien, P.; Rytz, G.; Momenteau, M.; Saveant, J.-M.; Xu, F. *J. Am. Chem. Soc.* **1984**, *106*, 4755–4765. (c) Lexa, D.; Maillard, P.; Momenteau, M.; Saveant, J.-M. *J. Am. Chem. Soc.* **1984**, *106*, 6321–6323.

Table V. Redox Potentials and Dioxygen Affinities for Some Ru(C6-PBP) Complexes

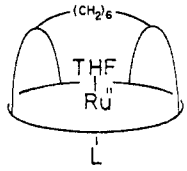

L	$E_{1/2}$ ($Ru^{III/II}$)*	O_2 Binding
1,5-DCI	+0.32v	+
PPh_3	+0.60v	–
PCy_3	+0.53v	–

* vs SSCE

Treatment of Ru(C6-PBP)$(THF)_2$ with 1,5-dicyclohexylimidazole (1,5-DCI), triphenylphosphine (PPh_3), or tricyclohexylphosphine (PCy_3) results in formation of the mixed-ligand complexes, Ru(C6-PBP)$(L)_{out}(THF)_{in}$ (L = 1,5-DCI, PPh_3, PCy_3). The regiochemistry of axial ligation in these molecules has been verified by treatment with pyridine, which replaces the labile THF ligand. The chemical shifts for coordinated pyridine in these complexes, by comparison to the bis(pyridine) complex, indicate regiospecific coordination of pyridine within the pocket.

When dry dioxygen gas is bubbled through a toluene solution of Ru(C6-PBP)$(1,5\text{-DCI})_{out}(THF)_{in}$, **11**, isosbestic spectral changes result that can be reversed on degassing with dinitrogen. These spectral changes are indicative of clean, reversible formation of a new species that we have characterized as a dioxygen adduct (see below). Interestingly, neither phosphine complex showed any affinity for dioxygen at atmospheric pressure as determined by visible spectroscopy. This is not a kinetic phenomenon as the THF ligand coordinated within the cavity was shown by ^1H NMR spectroscopy to be labile ($k_{diss} > 1.0 \times 10^{-3}$ at 25 °C). The low affinity of both phosphine complexes for molecular oxygen is consistent with the suggestion of Carter et al.[21] that dioxygen binding requires one-electron oxidation of the metal center. The Ru(III/II) redox potentials (vs SSCE) for the two phosphine derivatives are 210 and 280 mV positive of that for the imidazole complex as listed in Table V.

That formation of the dioxygen complex from Ru(C6-PBP)$(1,5\text{-DCI})_{out}(THF)_{in}$ could be completely suppressed by excess THF indicates dioxygen and THF are competing for the coordination site within the picnic-basket porphyrin cavity. This competition precludes direct measurement of a true equilibrium constant for dioxygen binding. Such a measurement requires that the five-coordinate complex, Ru(C6-PBP)$(1,5\text{-DCI})_{out}$, be prepared. Thus, a method was sought for generating an open coordination site within the picnic-basket porphyrin pocket.

An impure, five-coordinate ruthenium(II) porphyrin phosphine complex has been reported to result from zinc metal reduction of the corresponding ruthenium(III) halide.[22] Analogously, reduction of a ruthenium(III) picnic-basket porphyrin, with a halide bound regiospecifically within the pocket, should give a ruthenium(II) species with the desired open coordination site. One-electron oxidation of **11** with Ag^+ and treatment of the resulting Ru(III) species with $[Et_4N]Cl$ give Ru(C6-PBP)$(1,5\text{-DCI})_{out}(Cl)_{in}$, **14**, in high overall yield. This air-stable compound, characterized by elemental analysis, is easily purified by chromatography. Again, the regiochemistry of chloride binding in **14** was determined by tin metal reduction in toluene containing one drop of pyridine to form the previously prepared Ru(C6-PBP)$(1,5\text{-DCI})_{out}(pyr)_{in}$.

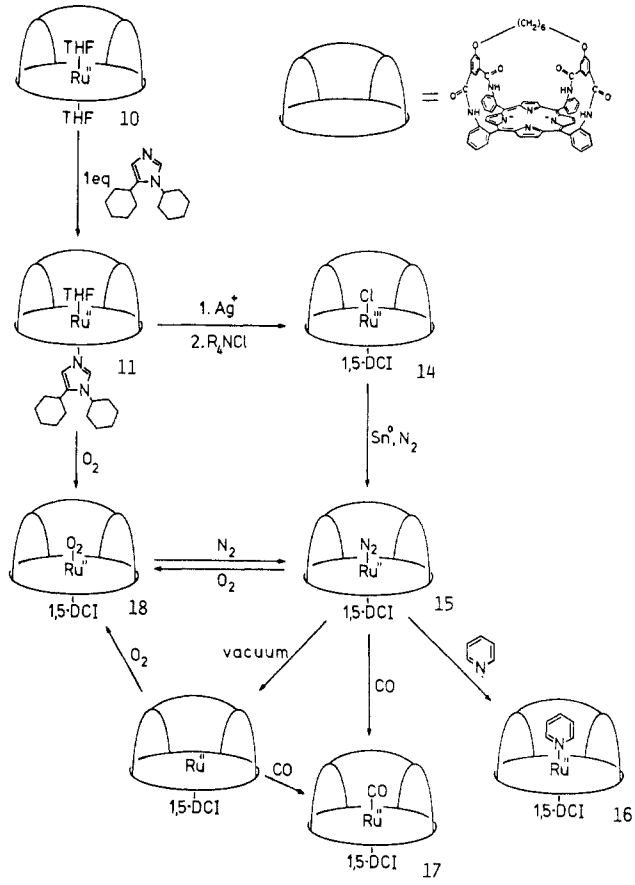

Figure 6. Ru^{III}(C6-PBP)$(1,5\text{-DCI})_{out}(Cl)_{in}$ synthesis and chemistry observed on reduction.

The synthesis of the ruthenium(III) complex and the chemistry observed upon its reduction are summarized in Figure 6. Reduction of **14** in dinitrogen-saturated toluene, in an inert-atmosphere box, resulted in formation of a new species, **15**, that has been characterized by its NMR, infrared, and visible spectra as a dinitrogen complex. The visible spectrum, with bands at 418, 507, and 533 nm, is similar to those of all six-coordinate ruthenium(II) picnic-basket porphyrins except the CO adducts. The NMR spectrum of a sample prepared in toluene-d_8 indicates a diamagnetic complex with easily recognized picnic-basket porphyrin signals and signals for coordinated 1,5-DCI. A strong infrared absorption at 2162 cm^{-1} was observed in both toluene and benzene solutions of this new species. A band in this region is indicative of coordinated dinitrogen; our measured value agrees well with those reported recently for a series of Ru(TMP)(L)(N_2) complexes.[8] If the dinitrogen stretching frequency is a measure of the back-bonding strength of the trans ligand, then a frequency of 2162 cm^{-1} with a trans imidazole ligand fits nicely within the series reported earlier.[8]

Although toluene solutions of the dinitrogen complex are stable for weeks in an inert-atmosphere box, the reactivity of the complex indicates the dinitrogen is labile and weakly coordinated. Exposure of a toluene solution of the dinitrogen adduct to pyridine, THF, CO, or O_2 leads quickly to the Ru(II) derivative in which dinitrogen has been replaced by the added ligand. Lyophilization of a benzene solution of the dinitrogen adduct gives an amorphous red-brown powder that has been tentatively identified as the five-coordinate Ru(C6-PBP)$(1,5\text{-DCI})_{out}$. Exposure of this powder to CO causes an immediate color change to cherry red, indicative of CO complexation. Examination of the infrared and NMR spectra of this red species shows that it is identical with the CO complex prepared in solution. The lyophilized powder, stored under vacuum, is not indefinitely stable and over several days decomposes to an unidentified paramagnetic material.

(21) (a) Carter, M. J.; Engelhardt, L. M.; Rillema, D. P.; Basolo, F. *J. Chem. Soc., Chem. Commun.* **1973**, 810–812.

(22) (a) James, B. R.; Mikkelson, S. R.; Leung, T. W.; Williams, G. M.; Wong, R. *Inorg. Chim. Acta* **1984**, *85*, 209–213. (b) James, B. R.; Dolphin, D.; Leung, T. W.; Einstein, F. W. B.; Willis, A. C. *Can. J. Chem.* **1984**, *62*, 1238–1245. (c) Sishta, C.; Camenzind, M. J.; James, B. R.; Dolphin, D. *Inorg. Chem.* **1987**, *26*, 1181–1182.

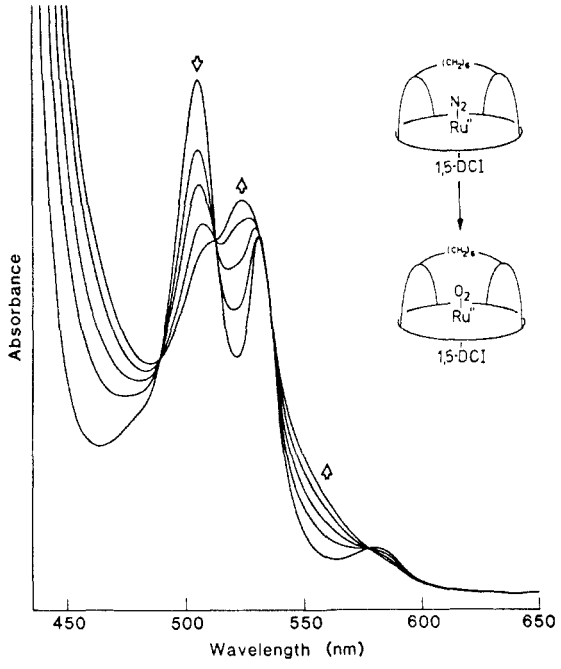

Figure 7. Visible spectrum changes observed as a toluene solution of $Ru(C6\text{-}PBP)(1,5\text{-}DCI)_{out}(N_2)_{in}$ is treated with O_2 gas.

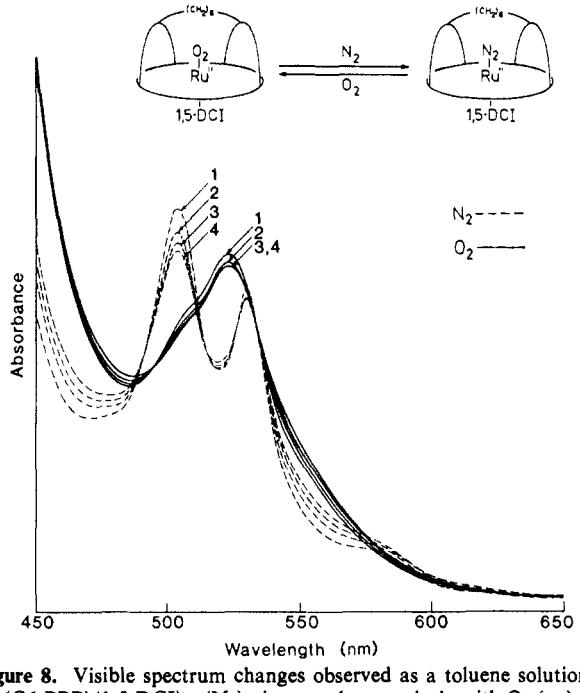

Figure 8. Visible spectrum changes observed as a toluene solution of $Ru(C6\text{-}PBP)(1,5\text{-}DCI)_{out}(N_2)_{in}$ is treated successively with O_2 (—) and N_2 (---).

Figure 7 illustrates the isosbestic spectral changes observed as dry dioxygen gas is bubbled through a toluene solution of the dinitrogen adduct. Complete conversion to the dioxygen complex, **18**, which we have characterized by visible, ^1H NMR, and infrared spectroscopies, requires approximately 15 min at 25 °C. Reversal of the above spectral changes could be effected by degassing with dry dinitrogen for 15 min and occurs with approximately 10% decomposition, as determined by decay of the visible bands. The dioxygen complex is metastable in toluene at room temperature under 1-atm O_2 pressure with a half-life of approximately 90 min. Slow irreversible oxidation to an unidentified paramagnetic species was observed. The visible spectra for four oxygenation/deoxygenation cycles are illustrated in Figure 8.

The room-temperature ^1H NMR spectrum of the dioxygen adduct was obtained by treating the toluene-d_8 solution of the dinitrogen adduct with dry dioxygen. Clean formation of a new

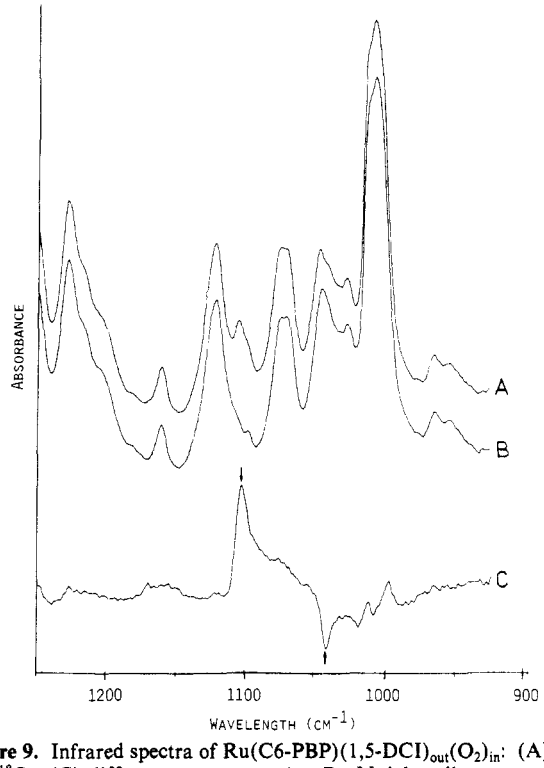

Figure 9. Infrared spectra of $Ru(C6\text{-}PBP)(1,5\text{-}DCI)_{out}(O_2)_{in}$: (A) $^{16}O_2$; (B) $^{18}O_2$; (C) difference spectrum, A − B. Nujol mulls.

diamagnetic species was observed. By ^1H NMR spectroscopy at room temperature, the O_2 complex maintains the effective C_{2v} symmetry of the C6-PBP. Therefore either the Ru–O_2 unit is cylindrically symmetric or rotation about the Ru–O_2 bond is rapid on the NMR time scale. No attempt was made to obtain the NMR spectrum at lower temperatures. The chemical shift of the signal assigned to the amide protons in the dioxygen adduct is very similar to that in both the carbonyl and dinitrogen complexes. Mispelter and associates[23] have reported very different amide proton chemical shifts in the dioxygen and carbonyl adducts of ferrous basket-handle porphyrins. Such shifts were cited as evidence of hydrogen bonding between the amide protons and coordinated dioxygen.

Solid samples of the dioxygen adduct, as well as the isotopically labeled $^{18}O_2$ complex, can be prepared by exposing the lyophilized dinitrogen complex to 0.5 atm of the oxygen gas. Infrared spectra of these species are conveniently measured as Nujol mulls of the lyophilized powder. Figure 9 shows a portion of the infrared spectra of the $^{16}O_2$ and $^{18}O_2$ complexes. Below, the difference spectrum is displayed. As can be seen in the difference spectrum, all absorbances cancel except for a positive absorbance at 1103 cm^{-1}, assigned to the ^{16}O–^{16}O stretch, and a negative peak at 1041 cm^{-1}, assigned to the ^{18}O–^{18}O stretch. The observed 62-cm^{-1} shift on isotopic substitution is within 2 cm^{-1} of that calculated by Hooke's law, thus supporting the assignments. An O–O stretching frequency of 1103 cm^{-1} is indicative of dioxygen reduced by one electron to superoxide ion.[24]

The physical properties of the ruthenium picnic-basket porphyrin dioxygen complex are most consistent with an η^1-angular structure. The infrared spectrum shows coordinated dioxygen reduced to the level of superoxide ion. The electronic distribution of the dioxygen complex is therefore best described as Ru^{III}–O_2^-. The visible spectrum of the dioxygen adduct is very similar to that of the parent ruthenium(III) chloride, consistent with this formalism. The observed diamagnetism of $Ru(C6\text{-}PBP)(1,5\text{-}DCI)_{out}(O_2)_{in}$, however, indicates there are no unpaired electrons

(23) Mispelter, J.; Momenteau, M.; Lavalette, D.; Lhoste, J. *J. Am. Chem. Soc.* **1983**, *105*, 5165–5166.

(24) Collman, J. P.; Hegedus, L. S.; Norton, J.; Finke, R. *Principles and Applications of Organotransition Metal Chemistry*, 2nd ed.; University Science Books: Mill Valley, CA, 1987; p 200.

in this molecule; this strong spin pairing is also found in end-bound dioxygen complexes of iron porphyrins (including oxyhemoglobin)[25] and can be interpreted in terms of an additional bond between the metal and the internal oxygen atom.

Experimental Section

Materials. All solvents and materials were of reagent grade quality, purchased commercially and used without further purification, except as noted below. Dry, oxygen-free benzene, toluene, and THF were distilled from benzophenone ketyl under dinitrogen and degassed with dinitrogen for 15 min. Benzyl isocyanide was purified by distillation under reduced pressure, and the dinitrogen and dioxygen gases used in the reversible spectral studies were obtained by passing the gas through 4-Å molecular sieves. The ruthenium picnic-basket porphyrin carbonyl complexes and ruthenium tetraphenylporphyrin bis(pyridine) complex were prepared as described previously.[12,15] 1,5-Dicyclohexylimidazole (1,5-DCI) was prepared by the method of Traylor et al.[26] Silica gel for flash chromatography was Type 7736, manufactured by E. M. Sciences and distributed by VWR Inc. For TLC, commercially prepared silica plates were purchased from Analtech Inc. All air-sensitive materials were handled by vacuum-line techniques or in a Vacuum Atmospheres drybox with MO-40 Dry Train capable of maintaining a nitrogen atmosphere with <2 ppm of O_2.

Physical Methods. Electronic spectra were obtained on a Varian Instruments Cary 219 spectrophotometer. Infrared spectra were measured on an IBM Instruments, Inc., IR/98 spectrometer as either methylene chloride solutions or Nujol mulls. Mass spectra were recorded at the Mass Spectrometry Resource, University of California, San Francisco, San Francisco, CA, and elemental analyses were obtained from Chemical Analytical Services, Berkeley, CA. A Nicolet NMC-300 or a Varian XL-400 spectrometer was used to record the NMR spectra. The high-temperature NMR spectra were obtained on the Nicolet instrument with use of the standard Nicolet constant-temperature controller. Samples of Ru(C6-PBP)(pyr)$_2$, dissolved in degassed pyr-d_5, were prepared in sealed NMR tubes. Just prior to its placement in the spectrometer, each NMR sample was preheated for 5 min in an oil bath maintained at a temperature 5–10 °C below that of the spectrometer. Each sample was allowed to equilibrate for 10 min in the spectrometer before data were collected for the next 2–3 h. At each temperature the NMR probe was calibrated with ethylene glycol, as described by Van Geet.[27] The integral decay was analyzed from simple first-order kinetics. The visible kinetic experiments were done on a 219 spectrophotometer in a thermostated cell maintained at constant temperature with a Braun Instruments Thermomix 1480 constant-temperature regulator. An *o*-dichlorobenzene solution of the ruthenium complex, in a septum-sealed cuvette, was equilibrated for 20 min in the spectrophotometer sample holder when 50–250 μL of preheated benzyl isocyanide was injected through the septum. The total solution volume in the cuvette was kept constant at 3.0 mL. The visible spectrum from 450 to 650 nm was monitored until no further change occurred. The visible spectral changes were analyzed by plotting ln $[(A_t - A_\infty)/(A_0 - A_\infty)]$ vs time, where A_0 is the initial absorbance at a convenient wavelength, A_∞ is the final absorbance at that wavelength, and A_t is the absorbance at intermediate times. A convenient wavelength for analysis is 505 nm. Electrochemical experiments were performed with a standard three-electrode cell and instrumentation on approximately 10^{-3} M porphyrin solutions in 0.2 M Bu_4NClO_4/CH_2Cl_2.

X-ray Data Collection and Structure Solution of Ru(C6-PBP)(pyr)$_2$. Suitable crystals of Ru(C6-PBP)(pyr)$_2$ were grown by vapor diffusion of toluene into a pyridine solution of the porphyrin at room temperature. The dark purple crystal selected for analysis was about 0.6 × 0.2 × 0.3 mm in size. Crystal data and collection details are given in Table II. The structure was solved by Patterson and direct methods[28,29] and refined by methods standard at Northwestern University.[29] No indication of disorder in the porphyrin superstructure was observed. The only complication was a pyridine solvate molecule disordered about an inversion center. Refinement of alternative positions with a variable occupancy factor was carried out. Prior to the final refinement on F, all hydrogen atom positions, except those of the disordered pyridine molecule, were idealized and their contributions were fixed. This final refinement involved 473 variables and 11 925 observations. Elaboration of the model, e.g., anisotropic refinement, was not attempted owing to the expense involved with minimal expectations of dramatic changes in the porphyrin parameters derived from these low-temperature data. Analysis of $\sum w(|F_o| - |F_c|)^2$ as a function of $|F_o|$, setting angles, and Miller indices revealed no unusual trends. Additional information on the refinement is given in Table II. Table 8S[18] lists the final positional and thermal parameters for the non-hydrogen atoms. Table 9S[18] lists the corresponding parameters for the hydrogen atoms. Table 10S[18] gives values of $10|F_o|$ vs $10|F_c|$.

Photolytic CO Replacement. Procedure 1 (L = Pyridine). Either regioisomer of Ru(PBP)(CO)(pyr) or more commonly a mixture (25 mg) was dissolved in 2 mL of dry pyridine in an NMR tube fitted with a stopcock. Three freeze/pump/thaw (FPT) cycles were performed on this solution. This solution was then irradiated with a medium-pressure Hg lamp for 4 h, and then two FPT cycles were performed. The 4-h irradiation followed by two FPT cycles was repeated twice more, and then the cooled solution was exposed to air. Workup involved removal of the pyridine solvent under vacuum and chromatography of the residue on silica gel (0.5-cm diameter × 4 cm) with use of a CH_2Cl_2 and then a 10% Et_2O/CH_2Cl_2 solvent gradient. Removal of solvent and drying the resulting residue under vacuum gave the desired product. Yield = 17.5 mg (83%) for Ru(C6-PBP)(pyr)$_2$.

Procedure 2 (L = THF, Pyridine). In an inert-atmosphere drybox 300 mg (0.24 mmol) of Ru(C6-PBP)(CO)$_{out}$(THF)$_{in}$ was dissolved in 250 mL of dry, degassed THF. This solution was transferred by cannula into an Ar-purged photolysis reactor. While the Ar purge was maintained, this solution was irradiated with a 450-W Hg lamp for 3 h, at which time the visible spectrum indicated the reaction was complete. The reaction solution was transferred by cannula into a clean, dry round-bottom flask under an Ar atmosphere, and this sealed flask was brought into a drybox. The solvent was removed under vacuum to yield the desired product in quantitative yield. Yield = 282 mg (92%) for Ru(C6-PBP)(THF)$_2$.

Ru(C6-PBP)(pyr)$_2$ (7). ^{1}H NMR ($CDCl_3$): δ 8.70 (d, 4 H), 8.42 (s, 4 H), 8.35 (d, 4 H), 8.12 (s, 4 H), 7.75 (t, 4 H), 7.59 (t, 4 H), 7.27 (s, 4 H), 6.71 (s, 4 H), 6.25 (t, 1 H), 6.10 (s, 2 H), 5.39 (t, 2 H), 4.03 (t, 2 H), 3.61 (t, 4 H), 2.95 (d, 2 H), 1.68 (d, 2 H), 1.46 (br m, 4 H), 1.12 (br m, 4 H). UV–vis (CH_2Cl_2): λ 412 (Soret), 505, 532 nm. MS: m/e = 1306 $(M)^+$ for $C_{76}H_{56}N_{10}O_6Ru$ (FD). Anal. Calcd for $C_{76}H_{56}N_{10}O_6Ru\cdot0.5CH_2Cl_2$: C, 68.16; H, 4.26; N, 10.40. Found: C, 68.56; H, 4.10; N, 10.43. The CH_2Cl_2 solvate was quantified by ^{1}H NMR spectroscopy.

Ru(C8-PBP)(pyr)$_2$ (8). ^{1}H NMR ($CDCl_3$): δ 8.85 (d, 4 H), 8.48 (s, 4 H), 8.28 (d, 4 H), 8.06 (s, 4 H), 7.91 (s, 4 H), 7.76 (t, 4 H), 7.57 (t, 4 H), 6.95 (s, 4 H), 6.62 (s, 2 H), 6.215 (t, 1 H), 5.36 (t, 2 H), 4.84 (t, 1 H), 3.78 (t, 2 H), 3.65 (t, 4 H), 2.86 (d, 2 H), 1.89 (d, 2 H), 1.46 (m, 4 H), 0.9–1.1 (br m, 8 H). UV–vis (CH_2Cl_2): λ 412 (Soret), 505, 533 nm. Anal. Calcd for $C_{78}H_{60}N_{10}O_6Ru\cdot0.5CH_2Cl_2$: C, 68.52; H, 4.48; N, 10.18. Found: C, 69.02; H, 4.47; N, 9.93.

Ru(PXY-PBP)(pyr)$_2$ (9). ^{1}H NMR ($CDCl_3$): δ 8.58 (d, 4 H), 8.39 (s, 4 H), 8.30 (d, 4 H), 8.04 (s, 4 H), 7.74 (t, 4 H), 7.56 (t, 4 H), 7.34 (s, 4 H), 6.97 (s, 8 H), 6.23 (t, 1 H), 6.10 (s, 2 H), 5.37 (t, 2 H), 4.91 (s, 4 H), 3.41 (t, 2 H), 2.95 (d, 2 H), 2.51 (t, 1 H), 1.56 (d, 2 H, buried under H_2O peak). UV–vis (CH_2Cl_2): λ 413 (Soret), 505, 532 nm. Anal. Calcd for $C_{78}H_{52}N_{10}O_6Ru\cdot CH_2Cl_2$: C, 67.22; H, 3.86; N, 9.93. Found: C, 67.00; H, 3.71; N, 9.69.

Ru(C6-PBP)(THF)$_2$ (10). ^{1}H NMR (THF-d_8): δ 8.45 (s, 4 H), 8.40 (s, 4 H), 8.22 (d, 4 H), 8.07 (s, 4 H), 7.96 (s, 4 H), 7.65 (t, 4 H), 7.51 (t, 4 H), 6.69 (s, 2 H), 6.65 (s, 4 H), 3.57 (t, 4 H), 1.03 (br m, 4 H), 0.62 (br m, 4 H), −2.33 (br m, 4 H, THF-d_8 exchangeable), −2.72 (br m, 4 H, THF-d_8 exchangeable). UV–vis (THF): λ 409 (Soret), 503, 530 nm. Anal. Calcd for $C_{74}H_{62}N_8O_8Ru$: C, 68.77; H, 4.84; N, 8.67. Found: C, 66.81; H, 4.63; N, 8.54.

Ru(C6-PBP)(1,5-DCI)$_{out}$(THF)$_{in}$ (11). In a drybox, 108 mg (84 μmol) of Ru(C6-PBP)(THF)$_2$ was dissolved in 3 mL of dry, oxygen-free THF. To this solution was added 45 mg (250 μmol) of 1,5-dicyclohexylimidazole, and the resulting mixture was stirred for 4 days. Reaction was monitored by removing the solvent from a reaction aliquot and examining the NMR spectrum of the residue dissolved in THF-d_8. When the reaction was complete by NMR analysis, removal of the solvent and drying the residue under vacuum gave the desired product, contaminated

(25) (a) Collman, J. P.; Gagne, R. R.; Halbert, T. R.; Marchon, J.-C.; Reed, C. A. *J. Am. Chem. Soc.* **1973**, *95*, 7868–7870. (b) Collman, J. P.; Brauman, J. I.; Suslick, K. S. *J. Am. Chem. Soc.* **1975**, *97*, 7185–7186. (c) Collman, J. P.; Gagne, R. R.; Reed, C. A.; Halbert, T. R.; Lang, G.; Robinson, W. T. *J. Am. Chem. Soc.* **1975**, *97*, 1427–1439. (d) Collman, J. P.; Brauman, J. I.; Halbert, T. R.; Suslick, K. S. *Proc. Natl. Acad. Sci. U.S.A.* **1976**, *73*, 3333–3337. (e) Collman, J. P.; Gagne, R. R.; Reed, C. A.; Robinson, W. T.; Rodley, G. A. *Proc. Natl. Acad. Sci. U.S.A.* **1974**, *71*, 1326–1329. (f) Linard, J. E.; Ellis, P. E.; Budge, J. R.; Jones, R. D.; Basolo, F. *J. Am. Chem. Soc.* **1980**, *102*, 1896–1904.

(26) Traylor, T. G.; Tsuchiya, S.; Campbell, D.; Mitchell, M.; Stynes, D.; Koga, N. *J. Am. Chem. Soc.* **1985**, *107*, 604–614.

(27) Van Geet, A. L. *Anal. Chem.* **1968**, *40*, 2227.

(28) Beurskens, P. T.; Bosman, W. P.; Doesbury, H. M.; Gould, R. O.; van den Hark, Th. E. M.; Prick, P. A. J.; Noordik, J. H.; Stempel, M.; Smits, J. M. M. Technical Report 1984/1, Crystallography Laboratory, Toernooiveld, 6525 Ed Nijmegen, The Netherlands.

(29) Waters, J. M.; Ibers, J. A. *Inorg. Chem.* **1977**, *16*, 3273–3277.

by approximately 1 equiv of 1,5-DCI but pure enough for the next step.

^{1}H NMR (THF-d_8): δ 8.46 (d, 4 H), 8.22 (s, 4 H), 8.08–8.06 (m, 8 H), 7.79 (s, 4 H), 7.61 (t, 4 H), 7.46 (t, 4 H), 7.28 (s, 1,5-DCI), 6.73 (s, 2 H), 6.70 (s, 4 H), 6.46 (s, 1,5-DCI), 3.61 (t, 4 H), 1.6–1.9 (br m), 1.05–1.35 (br m), 0.65–0.85 (br m). UV-vis (CH_2Cl_2): λ 413 (Soret), 504, 531, 582 (sh) nm.

Ru(C6-PBP)(PPh$_3$)$_{out}$(THF)$_{in}$ (12). In a drybox, a solution of 25 mg (20 μmol) of Ru(C6-PBP)(THF)$_2$ dissolved in 10 mL of 10/1 CH_2Cl_2/THF was stirred at room temperature for 24 h with 30 mg (1 mmol) of triphenylphosphine. This solution was removed from the drybox and reduced on a rotovap. The residue, dissolved in CH_2Cl_2, was chromatographed on silica with use of CH_2Cl_2 to elute unreacted phosphine and then 10/1 CH_2Cl_2/THF to elute the desired product. Removal of the solvent and drying the residue under vacuum gave the desired product. Yield = 27 mg (95%).

^{1}H NMR ($CDCl_3$): δ 8.67 (d, 4 H), 8.53 (s, 4 H), 8.05 (d, 4 H), 7.96 (s, 4 H), 7.78 (t, 4 H), 7.58 (t, 4 H), 7.52 (s, 4 H), 6.98 (t, 3 H), 6.81 (s, 4 H), 6.68 (t, 6 H), 6.56 (s, 2 H), 4.51 (t, 6 H), 3.55 (t, 4 H), 1.20–1.30 (br m, 4 H), 0.75–0.85 (br m, 4 H). UV-vis (CH_2Cl_2): λ 406 (sh), 424 (Soret), 507, 534 nm. Anal. Calcd for $C_{88}H_{69}N_8O_7PRu$: C, 71.29; H, 4.69; N, 7.56. Found: C, 70.97; H, 4.54; N, 7.46.

Ru(C6-PBP)(PCy$_3$)$_{out}$(THF)$_{in}$ (13). This compound was prepared by the above procedure, substituting tricyclohexylphosphine for triphenylphosphine.

^{1}H NMR ($CDCl_3$): δ 8.73 (d, 4 H), 8.70 (s, 4 H), 8.20 (d, 4 H), 7.84 (s, 4 H), 7.78 (t, 4 H), 7.59 (t, 4 H), 7.43 (s, 4 H), 6.85 (s, 4 H), 6.61 (s, 2 H), 3.56 (t, 4 H), 1.15–1.45 (br m), 0.8–0.9 (br m, 4 H), 0.25–0.70 (br m), −1.10 to −1.30 (br m), −1.70 to −2.00 (br m). UV-vis (CH_2Cl_2): λ 407 (sh), 423 (Soret), 507, 535 nm. No satisfactory elemental analysis was obtained for this compound.

Ru(C6-PBP)(1,5-DCI)$_{out}$(Cl)$_{in}$ (14). In a drybox, 108 mg of Ru(C6-PBP)(1,5-DCI)$_{out}$(THF)$_{in}$/1,5-DCI mixture prepared previously was dissolved in 50 mL of dry, oxygen-free toluene containing 2 mL of THF. To this solution was added 25 mg (0.13 mmol) of $AgBF_4$ dissolved in 10 mL of toluene. A precipitate was observed immediately on mixing but the solution was stirred for 0.5 h and then filtered through packed Celite. The Celite pad was washed liberally with toluene, the receiving flask changed, and the Ru(III) complex washed from the Celite with a 20:1 CH_2Cl_2–THF solution. The solvent was removed from the filtrate under vacuum and the residue dissolved in 30 mL of CH_2Cl_2 solution containing 0.2 g of [Et_4N]Cl. This solution was stirred for 4 h, removed from the drybox, and reduced to a solid on a rotovap. The residue was dissolved in CH_2Cl_2 and chromatographed on silica gel (10 cm × 4-cm diameter) with use of CH_2Cl_2 to 10/1 CH_2Cl_2/Et_2O as the solvent gradient. A deep red-brown band was isolated and the solvent was removed under vacuum to give the desired product. Analytical-quality crystals were obtained by layering benzene on a $CHCl_3$ solution of the Ru(III) complex. Yield = 87 mg (80%).

^{1}H NMR ($CDCl_3$): paramagnetic. UV-vis (CH_2Cl_2): λ 419 (Soret), 527 nm. Anal. Calcd for $C_{81}H_{70}N_{10}O_6RuCl\cdot0.5CHCl_3$: C, 66.33; H, 4.82; N, 9.49. Found: C, 66.19; H, 4.75; N, 9.52. $CHCl_3$ was observed in NMR spectrum of a THF-d_8 sample and was quantified in the reduced product.

Ru(C6-PBP)(1,5-DCI)$_{out}$(N$_2$)$_{in}$ (15). In a drybox, 10 mg of the Ru(III) precursor was dissolved in 5 mL of dry, N_2-saturated toluene or benzene. Granular tin metal (100 mg), previously activated by washing with dilute HCl and dried under vacuum, was added and the solution was stirred vigorously for 2 h, at which time the visible spectrum indicated complete reduction to a Ru(II) species. Often a porphyrinic precipitate was observed. From preliminary characterization, we believe this to be a less soluble toluene solvate of the Ru(III) precursor. After the solution had been stirred for 2 h, it was passed through a glass wool plug to remove any particulate matter. The dinitrogen complex was not isolated but was used as a toluene or benzene solution.

^{1}H NMR (toluene-d_8): δ 9.19 (d, 4 H), 8.66 (s, 4 H), 8.28 (s, 4 H), 8.25 (d, 4 H), 7.60 (t, 4 H), 7.43 (s, 4 H), 7.34 (t, 4 H), 6.80 (s, 4 H), 6.26 (s, 2 H), 2.82 (t, 4 H), 2.28 (s, 1 H), 1.94 (s, 1 H), 1.46 (s, 1 H), 0.80–1.35 (br m), 0.63 (m, 4 H), 0.20–0.60 (m), 0.00–0.15 (m), −0.25 to −0.10 (m). UV-vis (toluene): λ 418 (Soret), 507, 533 nm. IR: (benzene or toluene) 2162 cm^{-1}.

Ru(C6-PBP)(1,5-DCI)$_{out}$(pyr)$_{in}$ (16). Addition of a drop of pyridine to a solution of the above dinitrogen adduct resulted in rapid replacement of the coordinated dinitrogen by pyridine. Alternatively, reduction of the ruthenium(III) chloride complex in the presence of pyridine yields the pyridine adduct. Removal of the solvent, followed by chromatography on silica gel (eluent = 10/1 CH_2Cl_2/Et_2O) gave the pure compound.

^{1}H NMR ($CDCl_3$): δ 8.57 (d, 4 H), 8.32 (s, 4 H), 8.26 (d, 4 H), 7.98 (s, 4 H), 7.73 (t, 4 H), 7.56 (t, 4 H), 7.47 (s, 4 H), 6.72 (s, 4 H), 6.23 (s, 2 H), 4.69 (t, 1 H), 4.04 (t, 2 H), 3.63 (t, 4 H), 2.53 (s, 1 H), 1.99 (d, 2 H), 1.88 (s, 1 H), 1.35–1.55 (br m), 1.05–1.15 (br s, 4 H), 0.75–1.00 (br m), 0.10–0.35 (br m, 4 H). UV-vis (toluene): λ 411 (Soret), 505, 533 nm.

Ru(C6-PBP)(1,5-DCI)$_{out}$. A benzene solution of the dinitrogen complex was sealed in a lyophilization flask inside a drybox. The sealed flask was removed from the box and quickly frozen in liquid nitrogen. The flask was then evacuated and the frozen benzene solvent removed by sublimation. During the lyophilization, the flask was cooled in an ice/water bath. Removal of all the benzene left a fluffy red-brown powder that was further dried for 1 h at room temperature and 1 × 10^{-4} Torr.

Ru(C6-PBP)(1,5-DCI)$_{out}$(CO)$_{in}$ (17). Bubbling CO gas through a solution of the dinitrogen adduct for 10 min resulted in complete conversion to the CO complex. Alternatively, exposure of the lyophilized dinitrogen adduct to CO gas resulted in immediate formation of the CO complex, which could be purified by chromatography on silica gel (eluent = 10/1 CH_2Cl_2/Et_2O).

^{1}H NMR ($CDCl_3$): δ 8.88 (s, 4 H), 8.67 (d, 4 H), 8.43 (s, 4 H), 8.35 (d, 4 H), 7.82 (t, 4 H), 7.62 (t, 4 H), 7.28 (s, 4 H), 6.75 (s, 4 H), 6.36 (s, 2 H), 3.48 (t, 4 H), 2.18 (s, 1 H), 1.55 (s, 1 H), 1.05–1.45 (br m), 0.96 (s), 0.60–0.85 (m), −0.10 to +0.10 (m). UV-vis (CH_2Cl_2): λ 398 (sh), 418 (Soret), 535, 570 (sh) nm. IR: (CH_2Cl_2) 1946 cm^{-1}.

Ru(C6-PBP)(1,5-DCI)$_{out}$(O$_2$)$_{in}$ (18). Dioxygen that had passed through 4-Å molecular sieves was gently bubbled through a toluene solution of the dinitrogen complex for 20 min. A thin glass tube was used to deliver the O_2 gas. Alternatively, a freshly prepared sample of the lyophilized dinitrogen complex was exposed to 0.5 atm of dry O_2 for 0.5 h.

^{1}H NMR (toluene-d_8): δ 9.29 (d, 4 H), 8.27 (s, 4 H), 8.13 (d, 4 H), 8.04 (s, 4 H), 7.55 (t, 4 H), 7.44 (s, 4 H), 7.26 (t, 4 H), 6.72 (s, 4 H), 6.37 (s, 2 H), 2.96 (t, 4 H), 2.49 (s, 1 H), 2.24 (s, 1 H), 1.93 (s, 1 H), 0.80–1.35 (br m), 0.45–0.60 (m), 0.25–0.40 (m), −0.10 to +0.10 (m). UV-vis (toluene): λ 416 (Soret), 423 nm. IR: (Nujol) 1103 cm^{-1}.

Summary

We describe here a general method to control axial ligation in the ruthenium picnic-basket porphyrins. This methodology has been utilized in the synthesis of both a dinitrogen and a dioxygen complex. This is the first stable dioxygen adduct of a ruthenium porphyrin characterized by a range of spectral techniques. These data indicate that the ruthenium picnic-basket porphyrin dioxygen complex is very similar to the η^1-dioxygen complexes reported for Cr(II),[30] Fe(II),[25] Co(II),[31] and Rh(II)[32] porphyrins. These metalloporphyrins have in common a single vacant coordination site, a propensity to become six-coordinate, and a relatively low single-electron oxidation potential. Since a stable five-coordinate ruthenium complex that reversibly binds oxygen has not yet been characterized,[22c] it is unclear whether true dioxygen equilibrium binding constants can be measured for the ruthenium picnic-basket porphyrins.

Acknowledgment. Support from the National Institutes of Health (Grants NIH GM17880-16 and NIH GM17880-17 to J.P.C. and Grant NIH HL-13157 to J.A.I.) and the National Science Foundation (Grant NSF CHE83-18512 to J.P.C.) is gratefully acknowledged. The Nicolet NMC-300 and Varian XL-400 spectrometers were purchased with funds from the National Science Foundation (Grants NSF CHE81-09064 and NSF CHE84-14329). Ms. Patricia Bethel and the University of California, San Francisco Mass Spectrometry Facility, supported by the National Institutes of Health (Grant RR01614), obtained all the mass spectral data reported. Dr. Takachi Michida, Mr. Jack Moriarty, and Mr. Dave Milan are gratefully acknowledged for synthetic help. We thank Dr. Robert Hembre and Mr. Philip Hampton for help in preparing the manuscript.

Registry No. 7, 113585-16-3; **8**, 113585-17-4; **9**, 113597-91-4; **10**, 113585-18-5; **11**, 113585-19-6; **12**, 113585-20-9; **13**, 113585-21-0; **14**, 113585-22-1; **15**, 113585-28-7; **16**, 113585-23-2; **17**, 113585-27-6; **18**,

(30) Cheung, S. K.; Grimes, C. J.; Wong, J.; Reed, C. A. *J. Am. Chem. Soc.* **1976**, *98*, 5028–5030.

(31) (a) Stynes, H. C.; Ibers, J. A. *J. Am. Chem. Soc.* **1972**, *94*, 1559–1562. (b) Stynes, H. C.; Ibers, J. A. *J. Am. Chem. Soc.* **1972**, *94*, 5125–5127. (c) Carter, M. J.; Rillema, D. P.; Basolo, F. *J. Am. Chem. Soc.* **1974**, *96*, 392–400. (d) Wayland, B. B.; Minkiewicz, J. V.; Abd-Elmageed, M. E. *J. Am. Chem. Soc.* **1974**, *96*, 2795–2801. (e) Doppelt, P.; Weiss, R. *Nouv. J. Chim.* **1983**, *7*, 341–344.

(32) (a) Wayland, B. B.; Newman, A. R. *J. Am. Chem. Soc.* **1979**, *101*, 6472–6473. (b) Wayland, B. B.; Newman, A. R. *Inorg. Chem.* **1981**, *20*, 3093–3097.

113597-92-5; Ru(C6-PBP)$(CO)_{out}(THF)_{in}$, 113585-10-7; Ru(C6-PBP)$(CO)_{out}(pyr)_{in}$, 113585-11-8; Ru(C8-PBP)$(CO)_{out}(pyr)_{in}$, 113585-12-9; Ru(PXY-PBP)$(CO)_{out}(pyr)_{in}$, 113585-13-0; Ru(C6-PBP)$(1,5\text{-DCI})_{out}$, 113585-14-1; $[Ru(C6\text{-PBP})(1,5\text{-DCI})_{out}(THF)_{in}]^+$, 113585-24-3; $[Ru(C6\text{-PBP})(1,5\text{-DCI})_{out}(PPh_3)_{in}]^+$, 113585-25-4; $[Ru(C6\text{-PBP})(1,5\text{-DCI})_{out}(PCy_3)_{in}]^+$, 113585-26-5; $Ru(TPP)(pyr)_2$, 34690-41-0.

Supplementary Material Available: Bond distances (Table 1S), bond angles (Table 2S), metric details on the toluene (Table 3S) and pyridine solvates (Table 4S), distances from pyridine inside the basket to basket atoms (Table 5S), positional and thermal parameters for the non-hydrogen atoms (Table 6S), dihedral angles (Table 7S), deviations from the mean porphyrin plane (Table 8S), hydrogen atom positional and thermal parameters (Table 9S) (14 pages); structure amplitudes (Table 10S) (49 pages). Ordering information is given on any current masthead page.

Proton Exchange and Nuclear Magnetic Resonance Line Broadening in Aromatic Nucleophilic Addition and Substitution

Radu Bacaloglu,* Clifford A. Bunton,* Giorgio Cerichelli,[1] and Francisco Ortega[2]

Contribution from the Department of Chemistry, University of California, Santa Barbara, California 93106. *Received June 5, 1987. Revised Manuscript Received December 22, 1987*

Abstract: Aromatic nucleophilic addition and substitution by OH^- (OD^-) in DMSO-d_6–D_2O or D_2O are for many nitrobenzenes, naphthalenes, and activated azines accompanied by extensive hydrogen exchange. However, substrates that readily form Meisenheimer complexes or overall substitution products are the least readily exchanged. With some overall substitutions exchange is greater in products than in unreacted substrate, which shows that exchange involves an intermediate on the reaction path between substrate and product, and it has also been identified in overall addition. This intermediate is believed to be a charge-transfer complex between a radical anion and $^\bullet OH$ or its anion, and it exchanges aromatic hydrogen with D_2O. Line broadening of the NMR proton signals of unreacted substrate can also be observed due to interaction between this complex and substrate. The complex slowly dissociates, giving very extensive line broadening, especially in less aqueous media, but in aqueous media it goes forward to products.

The generally accepted mechanism of aromatic nucleophilic substitution on activated arenes (**1**) in polar hydroxylic solvents involves rate-limiting ipso addition giving a σ or Meisenheimer complex (**2**), which rapidly forms **3** (Scheme I).[3]

Reinvestigation of nucleophilic additions and substitutions involving nitroarenes, azines, and their halo and arenesulfonate derivatives shows that this simple mechanism is inadequate, even for solvents of high water content, under conditions in which the overall reaction is first order with respect to substrate.[4,5] Two intermediates were seen spectrophotometrically en route to the Meisenheimer complex, and the rate and equilibrium constants of the individual steps were calculated by using a general treatment based on relaxation theory.[4,5]

The postulated intermediates are a π-complex (**4**) and a charge-transfer complex of an anion radical and OH (**5**) (Scheme II). Scheme II is simplified because **5** can also react in its deprotonated form.[4,5]

π-Complexes are possible intermediates in aromatic nucleophilic addition and substitution,[6] and anion radicals are formed by

Scheme I

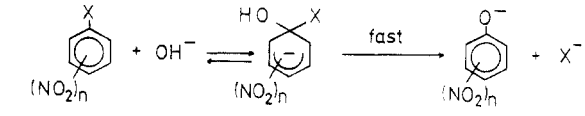

1 2 3

Scheme II

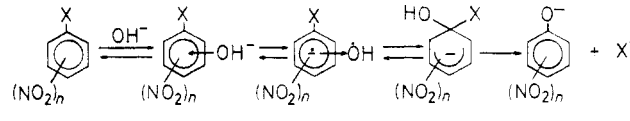

1 4 5 2 3

interaction of nitroarenes with bases, although usually in aprotic solvents of very low water content.[7] When we attempted to identify reaction intermediates by NMR spectroscopy, we saw loss of some aromatic proton signals, which was due both to exchange with D_2O of the solvent and to extensive line broadening,[4] and we therefore examined a number of nitroarenes and azines.

Aromatic compounds undergo base-catalyzed hydrogen exchange, and substrate deprotonation is postulated.[8] The position and rate of exchange can sometimes be correlated with inductive

(1) Present address: Institute of Organic Chemistry, University of Rome.
(2) The award of a NATO grant to F.O. is gratefully acknowledged.
(3) (a) Bunnett, J. F. *Q. Rev., Chem. Soc.* **1958**, *12*, 1. (b) Buncel, E.; Norris, A. R.; Russell, K. F. *Ibid.* **1968**, *22*, 123. (c) Strauss, M. J. *Chem. Rev.* **1970**, *70*, 667. (d) Bernasconi, C. F. *Chimia* **1980**, *34*, 1. (e) Terrier, F. *Chem. Rev.* **1982**, *82*, 78. (f) Illuminati, G.; Stegel, F. *Adv. Heterocycl. Chem.* **1983**, *34*, 305.
(4) Bacaloglu, R.; Bunton, C. A.; Cerichelli, G. *J. Am. Chem. Soc.* **1987**, *109*, 621.
(5) (a) Bacaloglu, R.; Bunton, C. A.; Ortega, F. *Int. J. Chem. Kinet.* **1988**, *20*, 195. (b) Bacaloglu, R.; Bunton, C. A.; Ortega, F. **1988**, *110*, 3503, 3512.
(6) (a) Ainscough, J. B.; Caldin, E. F. *J. Chem. Soc.* **1956**, 2528, 2540, 2546. (b) Allen, C. R.; Brook, A. J.; Caldin, E. F. *Ibid.* **1961**, 2171. (c) Miller, R. E.; Wynne-Jones, W. F. K. *Ibid.* **1959**, 2375; **1961**, 4886. (d) Liptay, W.; Tamberg, N. *Z. Electrochem.* **1962**, *66*, 59. (e) Kosower, E. M. *Prog. Phys. Org. Chem.* **1963**, *3*, 81. (f) Tamaru, K.; Ichikawa, M. *Catalysis by Electron Donor–Acceptor Complexes*; Wiley: New York, 1975; p 53.
(7) (a) Shein, S. M.; Bryukhovetskaya, L. V.; Pishchugin, F. V.; Starichenko, V. F.; Panfilov, V. N.; Voevodskii, V. V. *Zh. Strukt. Khim.* **1970**, 243. (b) Shein, S. M.; Bryukhovetskaya, L. V.; Ivanova, T. M.; *Izv. Akad. Nauk SSSR, Ser. Khim.* **1972**, 1543. (c) Bryukhovetskaya, L. V.; Mironova, L. V.; Shein, S. M. *Ibid.* **1973**, 1601. (d) Blumenfeld, L. A.; Bryukhovetskaya, L. V.; Fomin, G. V.; Shein, S. M. *Zh. Fiz. Khim.* **1970**, *44*, 931. (e) Abe, T.; Ikegami, Y. *Bull. Chem. Soc. Jpn.* **1976**, *49*, 3227; **1978**, *51*, 196.
(8) (a) Shatenshtein, A. I. *Adv. Phys. Org. Chem.* **1963**, *1*, 156. (b) Streitwieser, A.; Hammons, J. H. *Prog. Phys. Org. Chem.* **1965**, *3*, 41.

0002-7863/88/1510-3495$01.50/0